Mechanical Design of the VSR Cavity: An Elliptical 4-Cell 1.5 GHz SRF Cavity With Strong Waveguide HOM Damping for High-Current Accelerators

N. Wunderer, S. Fendinger, H.-W. Glock, F. Glöckner, J. Knobloch, E. Sharples-Milne, S. Scherer, A. Tsakanian, and A. Velez

***Abstract*—The mechanical design of an elliptical 1.5 GHz superconducting RF 4-cell cavity with strong waveguide higher order mode (HOM) damping is presented. It was developed in the variable storage ring project framework to serve as part of an upgrade for the synchrotron light source BESSY II operating at beam currents of up to 300 mA. This poses a great design challenge, demanding both: a system capable of extracting very high HOM powers (above 2 kW per cavity), the stresses arising during operation, and an overall cavity length of less than 1 m to fit into a given magnet lattice. As a result, a compact HOM waveguide-loaded cavity has been developed, fulfilling all the required criteria. The most remarkable feature of the cavity are the five waveguide extensions. The article describes the mechanical solutions adopted in the layout of the cavity with its subgroups. Special attention is given to numerical studies aiming for high pressure resistance whilst allowing for required tuning. A standardized pressure vessel code was not followed. Instead, a dedicated quality control procedure for manufacturing including ancillary material testing and welding qualification, was developed to allow for peak pressures of 3.5 bar(a) of the cooling medium. This article shows the successful mechanical design solutions developed to allow for the operation of such cavities in demanding operational regimes featuring both high gradients and strong beam currents. At time of writing, the first prototype is mechanically completed, and the first RF tests have been performed. Relevant manufacturing experiences which led to late-stage design modifications are included in this article.**

***Index Terms*—Cryogenic vessel, design engineering, manufacturing, material properties, mechanical engineering, mechanical simulation, niobium, safety analysis, superconducting radiofrequency cavity, synchrotron, ultrahigh vacuum flanges, waveguides.**

Received 31 January 2025; revised 28 March 2025; accepted 31 March 2025. Date of publication 3 April 2025; date of current version 2 May 2025. *(Corresponding author: N. Wunderer.)*

N. Wunderer, H.-W. Glock, F. Glöckner, E. Sharples-Milne, and A. Tsakanian are with the Helmholtz-Zentrum Berlin for Materials and Energy, 14109 Berlin, Germany (e-mail: nora.wunderer@helmholtz-berlin.de).

S. Fendinger and S. Scherer are with RI Research Instruments GmbH, 51429 Bergisch Gladbach, Germany.

J. Knobloch is with the Helmholtz-Zentrum Berlin for Materials and Energy, 14109 Berlin, Germany, and also with the University of Siegen, 57068 Siegen, Germany.

A. Velez is with the Helmholtz-Zentrum Berlin for Materials and Energy, 14109 Berlin, Germany, and also with the Technical University of Dortmund, 44227 Dortmund, Germany (e-mail: adolfo.velez@helmholtz-berlin.de).

Color versions of one or more figures in this article are available at https://doi.org/10.1109/TASC.2025.3557846.

Digital Object Identifier 10.1109/TASC.2025.3557846

I. Introduction

A. Environment and Design Targets

ELLIPTICAL multicell L-band superconducting RF (SRF) cavities are nowadays well-established devices based on more than three decades of development (e.g., [1], [2], [3]) but are mainly used in systems with low average beam currents. Setups with one or two elliptical cells are also successfully proven as harmonic cavities in synchrotrons and storage rings, up to Ampere-class currents. These are typically equipped with dielectric beam pipe higher order mode (HOM) absorbers operated at some spatial distance at room temperature (e.g., [4], more examples in [5]) or at a colder temperature level (e.g., at 80 K [6]). Beyond this, only a few designs with more than two cells were studied for applications generating average HOM power levels exceeding the capabilities of HOM couplers equipped with notch filters to block the accelerating mode. Such coupler or filter setups are typically limited by parasitic losses originating from fundamental mode fields at high-duty-cycle and high HOM power levels [7]. This prevents their application in high current storage rings or energy recovery linacs.

Suppose beam pipe space is not a limiting criterion. In that case, propagation of HOM power along beam pipes of large cross section toward mostly toroidal dielectric absorber sections is the most straightforward solution (cf. [8]). If length is limited, waveguides (WGs) attached as closely as possible to the elliptical cells is the only known cryo-compatible high-power HOM extraction method since they can handle high (kW-level), broadband RF power. The cross section of the waveguides needs to be chosen so that their lowest cut-off allows all parasitical HOMs to propagate outwards. Fields of the accelerating mode below cut-off, on the other hand, decay exponentially over the WG length, thereby limiting the impact of the WGs on the Q-value.

To the best of the authors' knowledge, the most advanced development in the field of waveguide-damped elliptical cells is described in [9], with a 5-cell cavity using two endgroups of three rectangular waveguide ports at both cavity ends. Those ports were built directly at the edge of the helium vessel, keeping the design very slim but putting the WG flange connections still in reach of non-negligible fundamental mode fields. A fundamental power coupling through one of the WGs was foreseen in the design. A prototype lacking a complete helium vessel was built

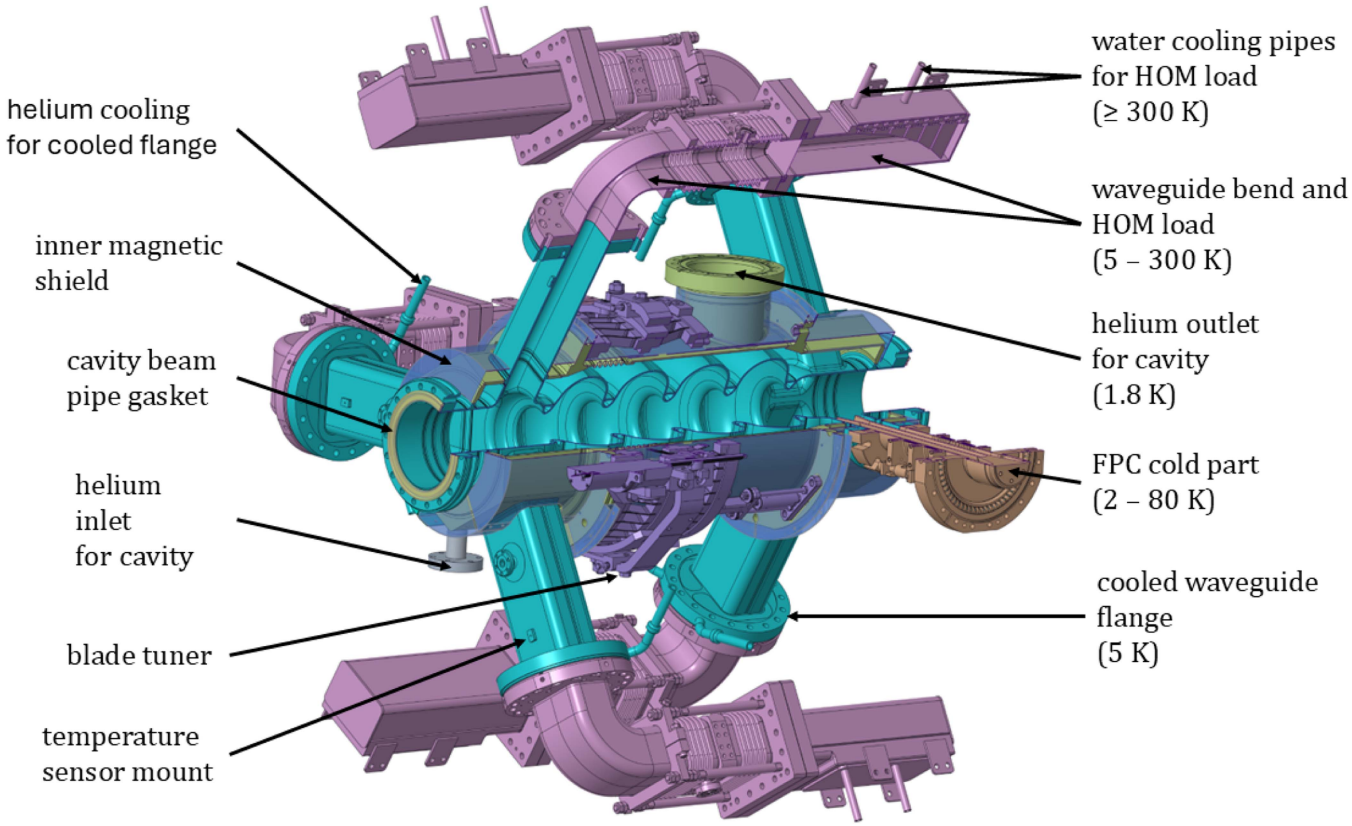

Fig. 1. Partially cut view of the VSR 1.5 GHz SRF cavity with superconducting niobium waveguides (turquoise) including helium vessel (green) and tuning system (purple) with ancillaries: waveguide bends, HOM loads (both pink), fundamental power coupler cold part (orange), and inner magnetic shield (semi-transparent blue).

TABLE I
BEAM PARAMETERS OF BESSY II

Parameter	Value
Circumference	240 m
Basic RF system (rounded)	500 MHz
Beam current (standard operation)	≤ 300 mA
No. of buckets	400

and vertically tested with successful results [10]. Nevertheless, the HOM damping and impedance performance does not meet the requirements for operation in a synchrotron machine such as BESSY II [11].

At Helmholtz-Zentrum Berlin (HZB), a potential upgrade of the third-generation light source BESSY II was pursued [11] to enable simultaneous storage of both long (∼15 ps) and short pulses (∼1.5 ps). BESSY II is a storage ring using an inhomogeneous filling pattern with a main gap and special high-charge bunches (main parameters summarized in Table I). A combination of 3rd and 3.5th harmonic cavities, each frequency operating at about 16 MV, was envisaged to generate a beating scheme to provide high and low voltage gradients in time at alternating RF buckets. Thus, both short and long pulses can be stored at the same time [12].

This triggered the development of a new SRF system in the framework of the BESSY variable pulse length storage ring (VSR) project, consisting of a cryomodule loaded with two 1.5 GHz 4-cell cavities (see Fig. 1, main cavity parameters in Table II) as described in this article (two prototypes currently in production), and two 1.75 GHz 5-cell cavities of similar design (only RF design complete). Indeed, the combination of very high currents in the synchrotron ring and the low impedance threshold required in the low beta straight available for installation, to avoid coupled bunch instabilities and beam break-up, pushed the design to go beyond the existing state of the art in damping performance and size reduction. Appropriate ancillaries such as HOM absorbers (developed in collaboration with Jefferson Laboratory (JLab) [13]) with connecting WG bends have been developed [14]. Cavity tuning is accomplished using a blade tuner [15]. Power is coupled with coaxial fundamental power couplers (FPCs) [16] following the Cornell high-current design [17]. While these devices have all been manufactured and are undergoing testing, they are not presented in this paper since the cavity mechanical design is the primary focus. However, the components represent critical boundary conditions and significantly influence the design solution adopted. Currently, a two-cavity demonstration module [18] with a spaceframe as a supporting structure is being built in the framework of the technology validation VSR DEMO project.

The dominating element of the cavity design is the WGs grouped in two different so-called endgroups. One side

TABLE II
CAVITY SPECIFICATION AND MAIN PARAMETERS

Parameter	Value
Operating mode	C.W.
Frequency	1.5 GHz
No. of cells	4
Operating voltage	8 MV
Accelerating gradient	20 MV/m
Total HOM power	≥ 2 kW per cavity
Required tuning range (freq.)	1 MHz
Tuning sensitivity	800 kHz/mm
Max. length (flange to flange)	765 mm
Beam pipe diameter	110 mm
Iris diameter	70.1 mm
Equator diameter	180.5 mm
Operating temperature	1.8 K
Operating liquid He pressure	16 mbar
Max. allowable He pressure	3.5 bar(a)

comprises of three such WGs, while the second endgroup comprises of two WGs plus a FPC port. The endgroups define a transition length almost of that of a cell. A large beam pipe diameter of 110 mm is chosen to reduce the beam impedance and to provide unhindered HOM propagation towards neighboring structures. Since, for some operational regimes of the storage ring, it must be possible to minimize the beam interaction of the cavities down to almost zero, detuning by a large value is required. Therefore, the cavity is designed to allow a mechanical tuning range of 1.5 mm, i.e., equivalent to over 1 MHz for operational tuning.

Nevertheless, to the best of the authors' knowledge, none of the worldwide existing cavity designs can handle both CW high-current and high-gradient while simultaneously fulfilling the RF and length specifications imposed by the use in BESSY II [11]. The high current cavity developed by JLab [10] represents a significant step forward but does not meet these specifications (e.g., HOM damping capabilities). Consequently, many new mechanical design challenges derived from the final RF geometries must be resolved. Since the high current cavity developed by JLab does not present a closed helium vessel, most of the mechanical demands remained unknown. As will be shown, vessel integration represents one of the major challenges of this cavity design.

In addition, the transparent operation of the cavities by detuning, i.e., the so-called parking, was another key challenge in the design process. Parking of the cavities in a cold state is demanding because of the large tuning range required, but possible due to the high material yield strength under cryogenic

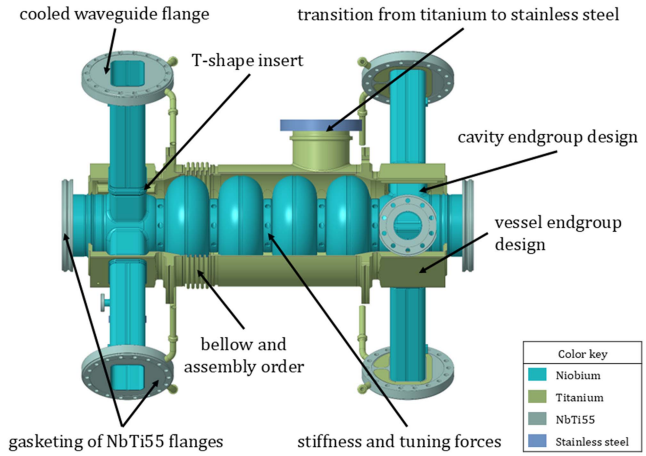

Fig. 2. VSR cavity with the components that pose the major technical design challenges labelled.

conditions. Warm parking is not a valid option since the cavity material will enter the plastic regime in this state. Another significant risk is the possibility of a tuner motor failure followed by a module warm-up in a detuned position. This will result in an irreversibly deformed cavity. To this end, further design and preventive measures have been studied and developed (cf. Section II-B.2).

B. Design Overview and Main Cavity Elements

An overview of the different cavity parts and the main mechanical design challenges is given in Fig. 2, these are introduced in this section. More detailed descriptions are given in the following sections.

The cavity cells, endgroups, and WG extensions are manufactured from niobium sheets. To provide superconductivity and to preserve sufficient hardness after the mandatory 800 °C annealing of the cavity, both beam pipe flanges, the FPC flange, and the two pick-up flanges are made of niobium-titanium (NbTi55). All vacuum gaskets are of aluminum in hexagon shape; beam pipe, FPC port, and WG gasket connections are additionally equipped with copper RF lips (cf. Section II-C). The cavity vessel, including the bellows, is made from titanium (Ti Grade 2). The flanges and pipes to connect the cooling media are made from stainless steel (316 LN ESR), and the transition from titanium to stainless steel (transition pipe 316 L) is achieved with explosive bonding.

The presented mechanical design is the consequent continuation of the final RF design optimizations described in [19]. The cavity body consists of two main parts: the cavity cells and the endgroups. The cell structure comprises three identical dumbbells and two identical end half cells. Half cells, endgroups, and WG extensions are manufactured by deep drawing. Close to the cell iris, stiffening rings are placed, reinforcing the cell connection, since overall bending stability was a substantial concern. The cavity endgroups consist each of two differently shaped half shells welded together. The WGs are arranged in 60° steps about the beam pipe, to best handle possible mode orientations whilst keeping symmetry. HOM spectra and cut-off considerations demand a large WG cross section of 91 mm x 60 mm. The

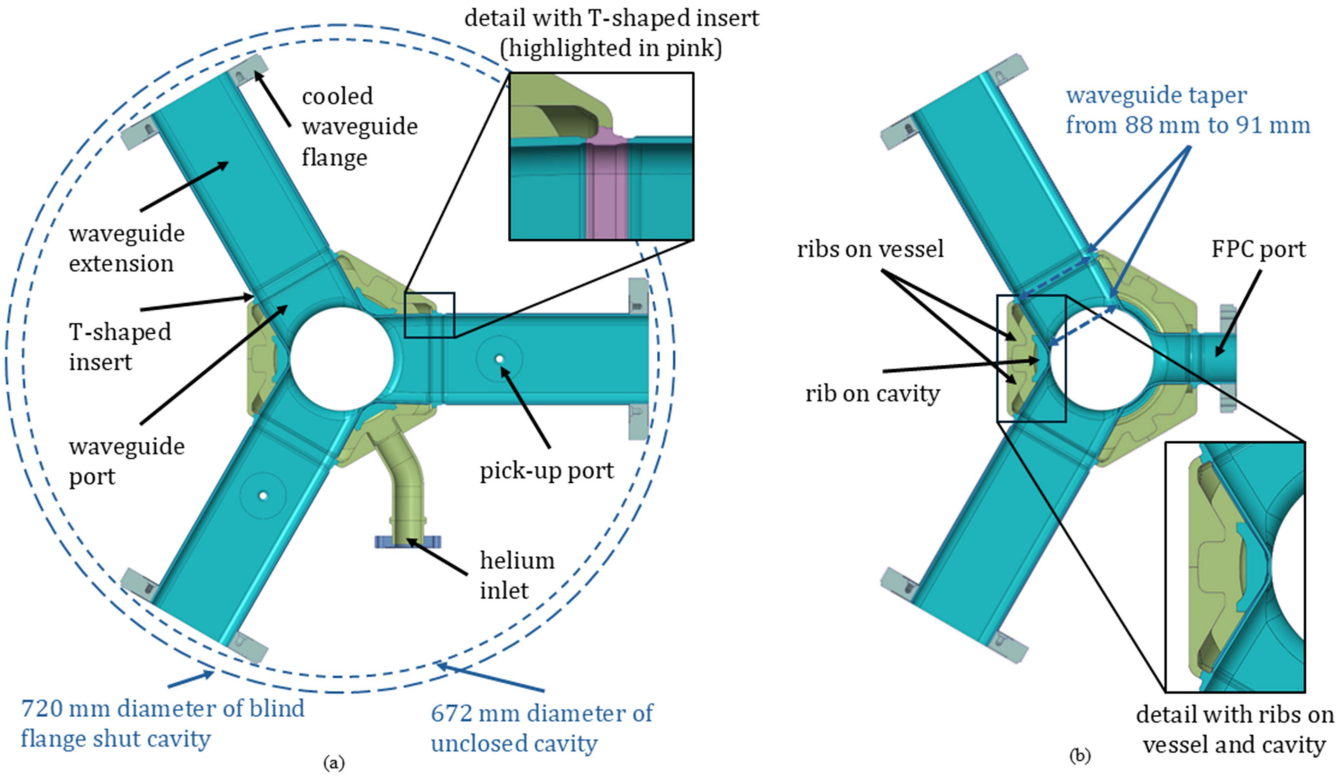

Fig. 3. Cut view of the cavity endgroups featuring (a) three waveguides (3WG) and (b) two waveguides and the coupler port (2WG1CP). Stiffening ribs on each vessel segment and on the cavity endgroups between each two WGs are shown.

height of the waveguides determines the cut-off for the modes that would otherwise not propagate due to their polarization [19]. One of the endgroups features the round FPC port instead of a third waveguide stud (see Fig. 3).

The WG extensions are continued by a 90° WG bend (cf. Fig. 1) having two bellows and a cooling intercept. The WG bends made from copper-plated steel connect the cavity with customized HOM loads (see Fig. 1). The cavity is designed to be operated at 1.8 K, whilst the HOM loads operate at around 300–350 K and are water-cooled to cope with deposited power levels of up to 460 W HOM power per load. Hence, the possibility of heat load transferring from the HOM load to the cavity quenching the superconducting WG extensions was a primary design concern. Consequently, the cavity's WG extensions outside the helium vessel are equipped with customized, actively cooled flanges (cf. Section II-C) since extending the helium vessel was not an option due to space limitations. The low field strength in this region allowed for higher temperatures (cf. [13]), so these flanges are connected to the 5 – 8 K cooling circuit. Dedicated mechanical testing of the flange was required, and more details, including gasketing, are found in Sections II-C and III-B.1.

The protruding WG extensions of over 200 mm in length result in an overall diameter of the blind flange shut cavity setup of 720 mm (see Fig. 3), making the cavity unwieldy and difficult to process in various manufacturing and testing stages. This complication was accepted to avoid parasitic RF losses in flange connections close to strong fundamental mode fields and not to hinder the conductive cooling of the WGs. The exterior piping of the cooling flanges is oriented to not further extend the space demands of the cavity. This is particularly important to provide accessibility for the cavity tuning machine and to limit other interferences during the production and mounting process.

Two of the waveguide extensions in the 3WG endgroup are equipped with a pick-up port [see Fig. 3(a)], one devoted to low level operation and the other to monitoring the HOM fields. In addition, all WGs are temperature monitored, featuring threaded holes for temperature sensor placement.

Fig. 4(a) shows the completed cavity before helium vessel integration ("undressed"), to be used for vertical testing and still allowing for slight frequency modifications by cell tuning. After a successful cold RF test, the cells and endgroups will be fully enclosed by a vessel for the liquid helium cooling bath [see Fig. 4(b)]. At each endgroup the helium vessel is composed of three milled titanium parts combining to a hexagonal cross section, plus a circular disc connecting to the beam pipe. Direct niobium-to-titanium welds mate cavity and vessel components, using particular intermediate parts (denoted as "T-shaped insert") at all such interfaces [cf. Fig. 3(a)]. Proper weld preparation and sequences are essential to limit distortions.

The FPC connection port extends from the endgroup, in a manner analogous to that of the WGs, and intersects the helium vessel. The FPC cold part flanged to the port has thermal intercepts at 5 and 80 K, and it is equipped with length-optimized bellows to reduce heat flow [16]. The warm part of the coupler operated at 300 K is placed outside of the module. Since the coupler intersects with the module and attaches directly to the cavity, it demands a fixed bearing of the cavity within the

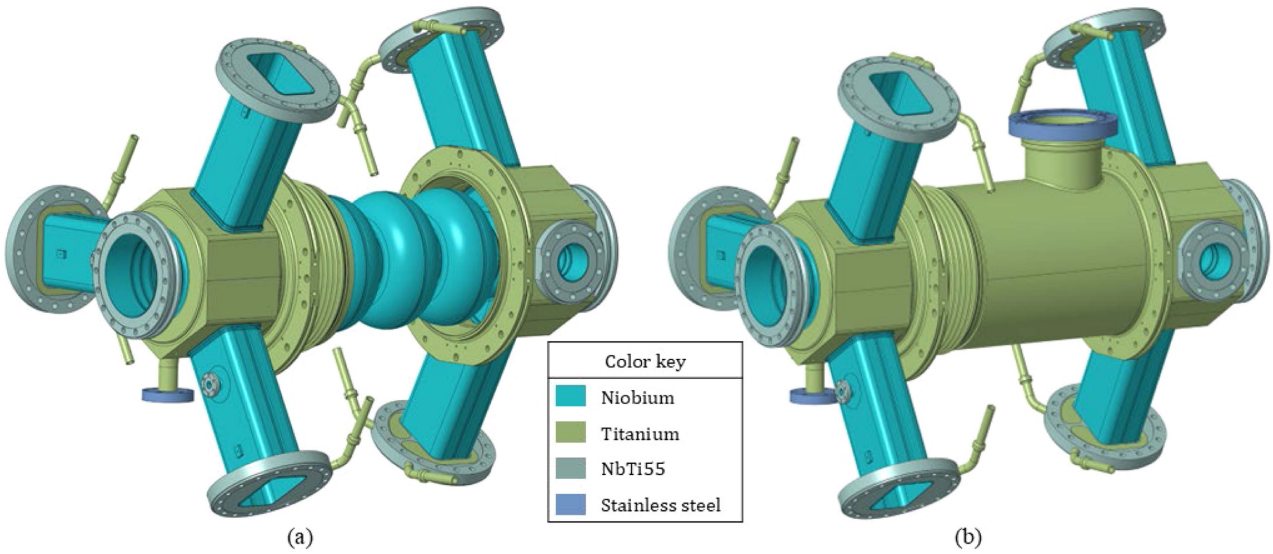

Fig. 4. 1.5 GHz VSR cavity in (a) undressed state, the bellows is movable and can be slid on either side to provide tuning access to the cells, and in (b) dressed state with integrated helium vessel.

cryomodule as close as possible to the FPC port. This is to ensure position stability and prevent shear-loading of the coupler during cool-down, that would be caused by thermal contraction of the cold string parts. Hence, the FPC port is the most important reference for cavity-in-module alignment.

Operational tuning demands longitudinal flexibility of at least 1.5 mm of the helium vessel, this is provided by a titanium bellows with an inner diameter of 214 mm integrated into the vessel. Since the bellows is located between the endgroups, it cannot be slid onto the cavity but it must be installed before completing the full cavity welding [see Fig. 4(a)]. A metal housing is used to protect the loose bellows until its final welding, i.e., during all further production, processing, and testing steps. Housing and bellows can be shifted along the cavity to give tuning access to all cells or can be attached to one or the other endgroup for fixation.

Two large flanges are integrated into the helium vessel (cf. Figs. 4 and 5) for connection of the blade tuner and the piezo elements used for slow and finetuning, respectively [15]. The required operational regimes of the cavity demand frequent tuning and large frequency shifts, simultaneously requesting a high tuning resolution of about 2 Hz/step. Therefore, the stepper motor employed for blade tuner actuation will need to operate nearly tenfold the number of steps guaranteed by the manufacturer. Reliability studies of the motor were performed [15]. However, a release mechanism is under development (cf. Fig. 5 for location), to save the cavity from plastic deformations in case of a stuck motor. This mechanism would allow for releasing the cold cavity from the tuner, warming up the cavity and the module, and replacing the motor (more details are provided in Section II-B.2 and [15]).

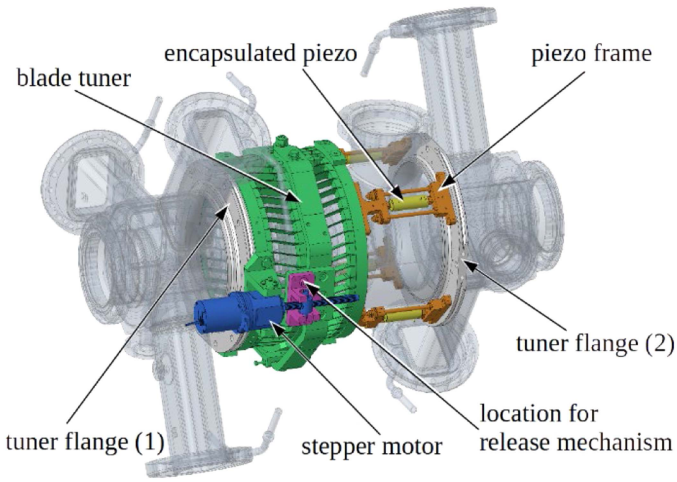

Fig. 5. Cavity with tuning system: a blade tuner driven by a stepper motor for coarse tuning, and four piezo elements in supporting frames for fast and fine tuning. Location of the release mechanism indicated on the blade tuner (pink).

C. Other Design Aspects and Chronology

The cavity's design needed to prioritize the required RF properties, which are accelerating mode parameters and HOM damping properties, while the mechanical design covering stability, reliability, and manufacturing aspects, remained secondary, imposing considerable challenges for the mechanical design process.

The rough chronological order of design progression was as follows: the cell parameters were fixed first [20], HOM calculations then defined cut-off requirements for the WGs [19]. This defines the boundary conditions for the fundamental mode decay along the WG extensions and a thermal balance between cavity, WG extension, WG bend, and HOM load [13]. Endgroup designs were drafted but revealed a conflict between structural stability and RF propagation properties (localized trapped modes, WG cross sections). This was resolved by applying a WG tapering inside the endgroups. Stiffening rings were introduced, and their size was optimized to compromise between acceptable tuning forces and sensitivity to pressure fluctuations. The

TABLE III
MATERIAL PROPERTIES EMPLOYED FOR DESIGN CALCULATIONS

Material	Cavity Parts	Density [kg/m³]	Poisson's Ratio [-]	Yield Strength [MPa]		Tensile Strength [MPa]		Young's Modulus [GPa]	
		293 K	293 K	293 K	2 – 4 K	293 K	2 – 4 K	293 K	2 – 4 K
NbTi55	flanges	6450	0.33	476	-	545	-	62.1	68.3
Ti Gr. 2	vessel, bellows	4510 [26]	0.36	275	834	344	-	106	117
Nb raw	-	8570	0.38	70	699	184	742	105	118
Nb heat treated	cells, endgroups, waveguides	-	-	38 [24]	317	114	600	-	-

Heat treated fine-grain niobium has received a 6 h bake-out at 800°C. Measured values are given in in TABLE V.

transition radii needed adjustment to provide sufficient pressure stability of the flat WG sections and the FPC port. Deep drawing of the endgroup shells revealed severe material thinning, which was compensated by stiffening ribs on the endgroup exterior. The design of the endgroup vessel elements finally followed the concept of the manufacturer RI Research Instruments GmbH (RI) but needed reinforcement to provide sufficient pressure stability.

Special attention was devoted to mitigating risks in the event of a fault to avoid damage to the cavity by plastic deformation, resulting from over-pressurization or occurring during warm-up combined with tuning. This was done in close connection to pressure vessel considerations. The cavity is classified as a pressure vessel category smaller than one, according to [21], and can be executed following the sound engineering practice as defined by German regulations. The process is certified by a third party (i.e., DEKRA Automobil GmbH, Halle) for external quality control, checking the design, material qualification, and the manufacturing (see Section III-B).

II. MECHANICAL DESIGN

The mechanical design had to find manufacturable solutions within the constraints of the RF design. In addition, the cavity must be stable for operational loads introduced by the cooling media or by tuning. The fine-grain niobium sheets of 3.1 mm nominal thickness with RRR 300 used for the cavity cells are mechanically weak. The material is chosen for its superconducting properties but is very soft and easily deformable. Literature indicates that the raw material yield strength is only 70 MPa at room temperature [22]. The temperature treatment of the assembled cavity at 800 °C required for hydrogen degassing causes further degradation of the mechanical stability [23]. Thus, Peterson et al. [24] recommend using a conservative value of only 38 MPa yield strength in the design process. All material properties used for design calculations are summarized in Table III.

Derived from the values in Table III, the max. allowable stress in the niobium structure must be lower than 38 MPa at room temperature. Good engineering practice usually requires safety factors of 1.3 to 2 for safety against plastic deformation and factors of 3 to 4 for safety against rupture. However, due to the low yield strength value and the limitations in design changes, safety factors of 1.1 for the elastic limit are accepted (max. allowable stress of 34.5 MPa), and safety against rupture should be 2 or higher (max. allowable stress of 57 MPa). For cold states, safety factors against plastic deformation of 1.5 (max. permissible stress of 211 MPa) and against rupture of 3 (max. permissible stress of 200 MPa) are to be met because in cold, the maximum loading is applied (pressure and tuning). While safety against the plastic limit must be held for any operational case of the cavity, safety against rupture is the criterion to be met for failure cases. This approach is necessary to allow for the max. release pressure of 3.5 bar(a), which was set at an early design stage of the cryo plant (cf. Section II-B).

Due to the constraints posed by the RF and scientific requirements on the system, the cavity's mechanical design safety offered only tight safety margins and had little room to maneuver. Therefore, a dedicated quality control scheme was implemented (cf. Section III), including room-temperature tensile tests of the niobium used for cavity production. The results of these tests and reassessment of the safety factors are found in Section III-B.

A. Cavity and Vessel Endgroup Design

The protruding WGs lead to an unusual design of the cavity endgroups, and of the helium vessel enclosing them, with the latter being the first of this kind to be built. Both the cavity and vessel endgroup require special attention during the manufacturing. While the former is challenging during the deep drawing steps, the latter requires attention during welding and impacts the possible assembly order. To reduce the number of flange connections to the cavity vacuum, the WG sections project directly from the cavity base to the WG bend. This reduces the number of flange connections per cavity by five compared to the JLab design [9].

One endgroup comprises three waveguides in an evenly spaced Y-shaped arrangement—abbreviated as the 3WG endgroup, while the other consists of two waveguides and a

tube to connect the FPC—abbreviated as 2WG1CP endgroup (cf. Fig. 3).

1) Cavity Endgroup: The beam tube segment's cross section and the WG cross section have been fixed at an early stage of the project [19]. The cavity endgroups transition axially from the dumb-bell end-cell shape to a circular beam pipe with an inner diameter of 110 mm. The WG extensions taper from 88 mm x 60 mm when exiting the beam pipe section to 91 mm x 60 mm at the T-shaped insert. This taper is geometrically necessary because the beampipe-base limits the size of the opening.

With a straight rectangular WG cross-section unwanted localized endgroup RF modes close to the fundamental mode frequency were trapped in the end-group region. To get rid of those modes a taper was introduced opening to the cross-section, as needed, for the propagation of all HOMs from the lowest dipole band. The size of the WG cross section on the base is mechanically limited to preserve a minimum quantity of material between WG and beam pipe. Thus, tapering between endgroup and T-shaped inserts was mandatory [25].

The first manufacturing experience showed a severe wall thickness reduction of the endgroup's niobium during the deep drawing process, to the point that pressure stability could no longer be guaranteed. To increase the pressure stability locally, reinforcing stiffening ribs are welded on the endgroup outside between the WG openings [cf. Fig. 3(b) and Section II-B.1].

2) Vessel Endgroup: The size of the vessel enclosing the cavity cells and the endgroups must find a compromise between two conflicting demands: on one hand, it must be as small as possible to minimize installation space, while on the other hand, it must cover as much of the niobium WG section to ensure superconductivity and foster cooling. For the vessel endgroup, different design options were assessed concerning stability, manufacturability, and required material amount. These options comprised hexagonal versus round shape, segmentation into three versus six parts per endgroup, and different arrangements of stiffening ribs on the segment between the WGs.

The vessel endgroup design was finalized in collaboration with the manufacturer RI, and the endgroup is built from three segments (see Fig. 6). Each segment is milled from a massive piece of titanium. Although this design requires a lot of material and milling work, the manufacturer favored it over a design consisting of six segments that would require far more welding steps with the associated heat-induced stress and distortion. Moreover, the outer shape remained hexagonal, while the inner contour is partially round. This shape increases pressure stability while decreasing the required material removal. Stiffening ribs are directly manufactured from the vessel plates during milling. And these ribs increase the moment of resistance against bending, hence increase pressure stability. The vessel endgroups are equipped with threaded holes on the outside to mount temperature sensors for diagnostic purposes. A round vessel shape on the outside was discarded—although ideal for a pressurized system—since connecting to the intersecting elements—i.e., WGs and FPC port—would become difficult.

The intersection of the WGs made from niobium with the vessel made from titanium was set to be formed by a niobium insert of a T-shape cross section. This insert sections the WGs or FPC port pipe, respectively, and allows for a well-performable and high-quality electron beam weld to the vessel plate. The direct weld of niobium to titanium requires special attention and qualification to fulfil the pressure vessel and leak tightness demands. RI as the manufacturer proposed to execute this weld directly between the two different materials since they have sufficient and good experience. Investigations have proven that there is no severe degradation of strength [27] and niobium remains the weakest part of the pressurized component.

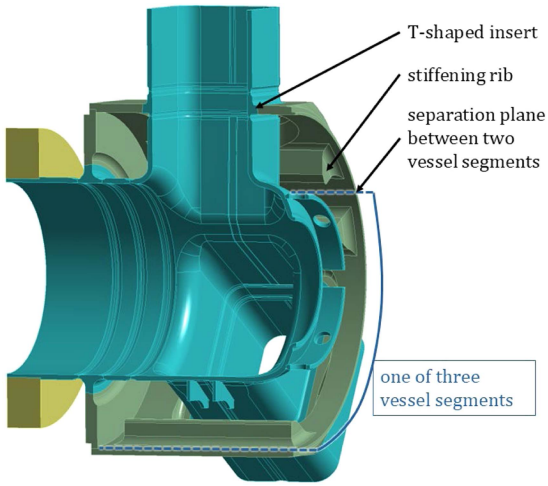

Fig. 6. Cavity and vessel endgroup in cut view showing details of the vessel segmentation and stiffening ribs.

B. Simulations and Design Optimizations for Loaded Conditions

The innovative cavity design required intense studies with simulations for various load cases. These load cases resemble the different states the cavity must withstand during assembly, testing, and operation and are summarized in Table IV. The load cases 4, 6, and 8 reflect worst-case loading, i.e., max. pressure, max. tuning or combinations. In addition, these conditions occur or can persist with the cavity at room temperature. Since niobium's strength is considerably lower at room temperature, compared to cryogenic temperature these cases must be considered as the most critical loading. The worst-case conditions can be described as follows.

1) Pretuning of the cavity during blade tuner installation at room temperature with the demand for no plastic deformations (case 4, Table IV)—more details in Section II-B.2.
2) Over pressurization: Due to a malfunction or a maloperation of the cryo-plant, over-pressurization in the helium system arises at room-temperature. The cavity is fully detuned to represent the worst case. This case is considered a failure scenario. Therefore, minor plastic deformations of the cavity would be accepted, but not a rupture. A cascade of safety valves opening at different pressure levels is integrated into the feedbox at the operating location, and more details are provided in the following section (cases 6, Table IV).

TABLE IV
CAVITY LOAD CASES DURING PRELIMINARY TESTING, ASSEMBLY, OPERATION, AND FAILURE CASES AND RESULTING PEAK STRESS

				Boundary and load condition				Result	
	Case no.	**Description**		**Iso. vac.**	**Cavity temperature**	**Max. pressure difference**	**Max. tuning**	**Resulting peak stress**	**Peak stress location**
undressed	1 a	Leak check		-	293 K	1 bar	0 mm	23 MPa	T-shape insert
	2 a	Vertical test	*Operation*	-	1.8 K	0.016 bar	0 mm	0.4 MPa	-
	2 b		*Cryo failure*	-	< 80 K	4 bar	0 mm	90 MPa	T-shape insert
	2 c		*Cryo plant maloperation*	-	293 K	1.05 bar	0 mm	24 MPa	T-shape insert
dressed	1 b	Leak check		-	293 K	1 bar	0 mm	23 MPa	T-shape insert
	2 d	Vertical test	*Operation*	-	1.8 K	0.016 bar	0 mm	0.4 MPa	-
	2 e		*Cryo failure*	-	< 80 K	4 bar	0 mm	90 MPa	T-shape insert
	2 f		*Cryo plant maloperation*	-	293 K	1.05 bar	0 mm	24 MPa	T-shape insert
	3 a	Horizontal test	*Operation*	Yes	1.8 K	0.016 bar	1.5 mm	291 MPa	Cell to stiff. ring
	3 b		*Cryo failure*	Yes	293 K	1.2 bar	1.5 mm	290 MPa	Cell to stiff. ring
	4	Pre-tuning		-	293 K	1 bar	0.15 mm	34 MPa	Cell to stiff. ring
	5	Cold operation		Yes	1.8 K	0.016 bar	1.5 mm	291 MPa	Cell to stiff. ring
	6 a	Cryo failure	*PLC driven safety valve opens*	Yes	1.8 – 293 K	1.5 bar	1.5 mm	289 MPa	Cell to stiff. ring
	6 b		*Small safety valve opens*	Yes	1.8 – 293 K	2.5 bar	1.5 mm	288 MPa	Cell to stiff. ring
	6 c		***Safety valve opens***	**Yes**	**< 80 K**	**3.5 bar**	**1.5 mm**	287 MPa	Cell to stiff. ring
	7	Break of isolation vacuum		-	1.8 – 293 K	0.016 – 3.5 bar	1.5 mm	287 MPa	Cell to stiff. ring
	8 a	Motor failure	***Motor release (cavity axially unsupported)***	**Yes**	**1.8 K**	**0.016 bar**	**1.5 mm**	291 MPa	Cell to stiff. ring
	8 b		*Cavity axially unsupported and warm-up*	Yes	1.8 – 293 K	0.5 bar	-	37 MPa	Cell to stiff. ring
	8 c		***Warm cavity axially unsupported and cryo fault***	**Yes**	**293 K**	**1.5 – 3.5 bar**	**-**	261 MPa	Cell to stiff. ring

Pressure difference refers to the value between cavity beam pipe and vessel or ambient pressure. Tuning indicates the max. possible tuning in that condition. Rows highlighted in grey (cases 4, 6b, 6c, 8a, 8b, and 8c) represent worst-case scenarios described in more detail in the following sections. Those cases that ultimately drove the design choice are highlighted with bold letters.

3) Break of the isolation vacuum: an abruptly broken isolation vacuum would cause sudden overload, leading to a fast warm-up and fast pressure increase in the helium system due to vaporization (case 7, Table IV). The consequence is a load case like case 6 c, Table IV.
4) The tuner motor breaks and is released: The cavity is fully detuned by 1.5 mm, then the traveling nut seizes on the motor spindle. To replace the motor, a cavity warm-up is required to access the failed component. Stress caused by the tuning exceeds the elastic limit of the cavity at room temperature. Hence, the release mechanism needs to be actuated, disrupting the connection between tuner and cavity (see Fig. 5) whilst still cold. The expansion of the then unbound cavity can be limited only by controlling the pressure of the helium system (cases 8, Table IV).

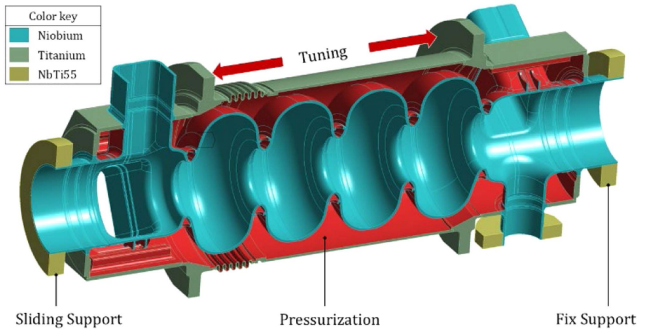

Fig. 7. Cavity half model with boundary conditions, i.e., supporting bearings, tuning force indicated with red arrows, pressure exposed surfaces marked in red, and material assignment (see box) as used for simulations.

a) Warm-up with a dedicated warm-up-scheme, pressure limited to 0.5 bar(a) (case 8 b, Table IV).
b) Warm-up with a fault and over pressurization of 3.5 bar(a) (case 8 c, Table IV).

A mirror-symmetry is given in the plane defined by the coupler and beam-pipe axis, ignoring the helium inlet and outlet port on the vessel. Simulations are performed in ANSYS Mechanical (ANSYS 2024 R1) on a half model, taking advantage of the symmetry to reduce calculation efforts (see Fig. 7). The cavity is supported at the beam pipe flanges, and tuning is introduced to the tuner flanges on the cavity vessel by the respective displacement (see Fig. 7). The WG extensions are partially excluded from the simulation since they do not impact the result.

Shape, size, and combined loading (pressurization and tuning) require a high mesh resolution, leading to unacceptably high computational time. Therefore, simulations were executed first with a coarse mesh on the whole model, from which three subsections were extracted: the two endgroups and the middle section of the cavity cells. Meshes on these submodels were refined in the areas of high stress to identify reliable peak stress values. In both endgroups, stress peaks occur in the contacting region of cavity and stiffening ring because of tuning forces. The results in both endgroups feature a singularity in this contact region, which cannot be circumvented even with further mesh refinement. Instead, the singularity with the overshooting result is excluded from the evaluation. And the nearly symmetrically loaded tip of the opposite stiffening ring half is evaluated and taken as the highest stress of the loaded zone.

1) Pressurization: To achieve a sufficiently high Q-value in operation, the cavity cells are cooled to 1.8 K. During cool-down and warm-up, the 1.8 K helium system is pressurized up to 1.05 bar(a), while normal operation is at 16 mbar. Pressure loads are applied to the cavity walls during testing and operation. Pressure above 1 bar(a) may originate in faults of the cryo plant providing the cooling medium. Vertical and horizontal cavity testing will be performed at HZB's large vertical test stand (LVTS) and horizontal bi-cavity testing facility (HoBiCat), respectively. Two different cryo plants feed these test stands, while operation will be executed with yet another cryo plant. All these plants had to be assessed with respect to their releasing pressures. The LVTS's safety valve max. release pressure is set

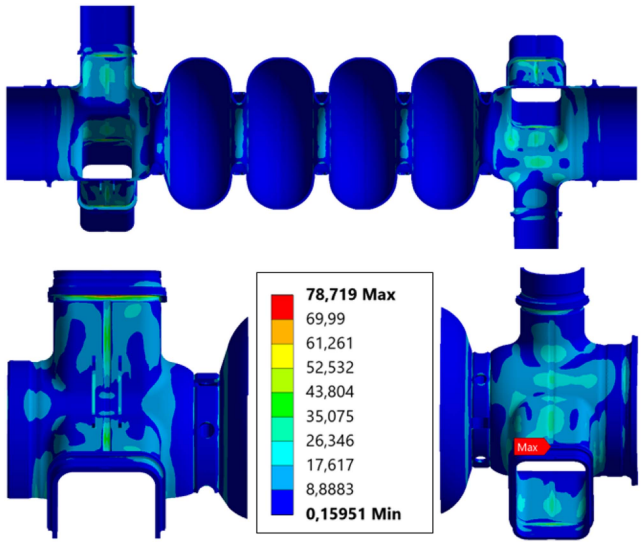

Fig. 8. Resulting stress in MPa from 3.5 bar(a) pressure loading of the untuned cavity with safety against rupture smaller than 2 if appearing at room temperature.

at 4 bar(a) and represents maximum pressure loading. Resulting peak stress values of around 90 MPa would be critical only at room temperature. This is an accepted risk, since only a very unlikely maloperation of the cryo plant could lead to such a case. More likely is a case of a cavity quench, with a cold and hence stronger cavity. After the quench and the sudden pressure increase the safety valve would close and the low-pressure system operating at 1.05 bar(a) would come back into operation.

The cooling circuit of the cryo plant designated for operation has a max. release pressure of 3.5 bar(a). But simulations of the pressurized cavity revealed unacceptably high stress values in the endgroups for such loading (see Fig. 8). Thus, a cascade of safety valves was implemented into the feedbox. The main safety valve opens at 3.5 bar(a) and can release the full mass flow. An additional valve opens at 2.5 bar(a) with limited mass flow release to prevent over-pressurization of the cavity at room temperature. A third PLC-driven valve opens at 1.5 bar(a), with limited mass flow release backing up these safety measures. The max. pressure of 3.5 bar(a) will not be experienced at room temperature, because the mass flow released by the valve with an opening pressure of 2.5 bar(a) would suffice. Full mass flow release is only required for an event at cryogenic temperature with a phase transition of the liquid helium phase to gas. Because of the high stress caused by the max. pressure and the cascaded safety valves, a dedicated quality control scheme for the manufacturing process was developed in cooperation with DEKRA as an inspection authority regarding pressure vessel standards.

The pressurized load cases lead to peak stress in the endgroups. This is because their shape, with many flat surfaces, is more pressure-sensitive than the nodular cells. Changes were required to limit this stress to values not exceeding the material's yield strength at room temperature (see Fig. 9). Simulations revealed that a change in radius of the WG corners from 5 to 10 mm would lower the stress sufficiently. This change was

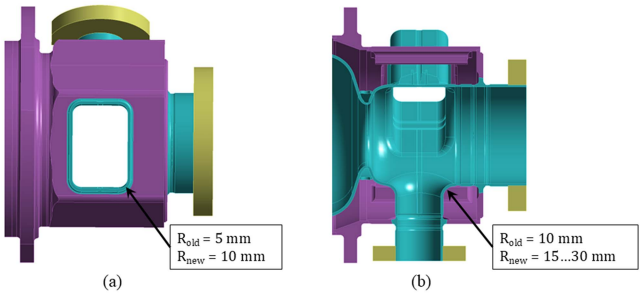

Fig. 9. Endgroup with design changes to reduce peak stress in critical regions. (a) Increased radius in the waveguide corners. (b) Increased and variable chamfer radius in the connecting area of FPC port and cavity endgroup.

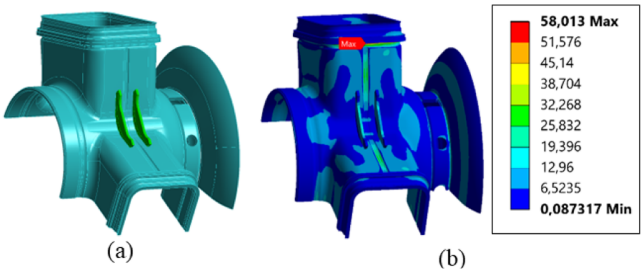

Fig. 10. 3WG cavity endgroup (a) as used for detail simulation, stiffening ribs highlighted in green. (b) Simulation result for pressurization with 2.5 bar (a) with the max. stress arising in the region of the T-shaped insert.

backed by RF simulations to prove that it would not impact on the waveguide's cut-off frequency.

Similarly, the transitioning radius between beam-pipe and coupler connection pipe was modified from the original value of 10 mm. Due to geometry and space limitations, a varying radius was introduced with a value of 15 mm in the longitudinal plane increased to 30 mm at the location of peak stress. The effect of this modification on the coupler performance was assessed, and a slight change of coupler tip length was required [28].

These simulations were based on a constant wall-thickness of the endgroups, even though it was clear that the highly complex shape of the endgroups would lead to significant thinning of the wall-thickness caused by material flow during the deep-drawing process. However, it is difficult to make sensible predictions of these variations. During the manufacturing process of the first three prototype endgroups, this effect was assessed, and minimum wall-thickness values down to 2.17 mm (before etching) were found in both endgroups in the region between two WG ports. These values were not acceptable since the simulation result computed with a constant wall-thickness of 2.8 mm (as designated wall-thickness after etching) only offered a safety factor against plastic deformation of 1. Therefore, stiffening ribs were added in agreement with the manufacturer [see Fig. 10(a)]. These provide an auxiliary connection between WGs and beam-pipe to release stress from the highly loaded areas. The transition to the coupler connection port is less inconvenient for deep-drawing, and on the manufactured parts, wall-thickness values of 2.86 mm or higher were measured in this region. Therefore, no ribs were introduced, but it was arranged for an adopted weld-preparation with less material removal. Simulations of the endgroups with wall thickness of only 2.4 mm, with stiffening ribs and pressurization with 3.5 bar(a), result in peak stress of 10 MPa in the discussed location and are hence not considered critical.

Instead, peak stress occurs in the T-shaped insert. During the design process of the vessel and the connection to the cavity, this aspect was studied intensely. The initial design with flat vessel plates introduced an even higher bending momentum because the flat vessel plates are sensitive to pressurization and deform outwards like the waveguide's flat surfaces. Peak stress occurs in a region already weakened by weld-preparations. To decrease this deformation and the resulting peak stresses in the WGs surpassing the yield limit, stiffening ribs on the vessel plate's inside were introduced. Simulations on various designs revealed that thicker vessel plates or a single rib per plate would not sufficiently reduce peak stresses. Therefore, two longitudinal ribs on each un-intersected vessel plate were added to the design, lowering the peak stress to acceptable values. The manufacturer then revised this intermediate design, as mentioned in Section II-A.2. The final design builds each vessel-endgroup by milling three solid titanium blocks, keeping a round shape at the inside where possible. This design and the adopted shape of the stiffening ribs with increased cross-section led to a higher section modulus. As a result, peak stress in the T-shaped insert is reduced to 58 MPa at 2.5 bar(a) pressurization [see Fig. 10(b)], hence achieving just the required safety factor.

The worst loading conditions appear during operation in a combined state of pressurization and tuning and are dominated by the effects caused by tuning.

2) Tuning: The stiffening ring position was revised from an initial design without rings with a high enough first mechanical eigenmode [29] to a design with a compromise between peak stress, required tuning forces, and sufficiently low detuning, f, versus pressure, p, (df/dp) stability. The stiffening ring diameter was adjusted from 108 to 95 mm to reduce peak stress close to the iris caused by tuning of the cavity [30]. The reduced diameter decreases the stiffness which leads to less required tuning force, roughly 80% force compared to rings with diameter of 108 mm and only 10% more force than a design without rings. The new ring position still offers a pressure stability of $df/dp = 9.8$ Hz/mbar to fluctuations in the helium bath [31]. The tuning sensitivity is calculated to be 800 kHz/mm. This was the compromise accepted, easing cavity safety and tuner operation.

The required tuning range of 1.5 mm (including some overhead for changed tuning sensitivity) challenges the cavity's stability while demanding great forces and high stiffness of the tuning system. The extensive tuning range results from operational demands (see Fig. 11): the VSR operation mode, with the cavities tuned very closely to their resonant frequency; and the parking mode, with the pair of cavities tuned in opposite frequency shift off-resonance. If no interaction is required, the parking mode allows the cavities to be transparent to the beam. To achieve this mode, a tuning range of about 1 MHz is needed.

A blade tuner was engineered in collaboration with LASA/INFN will provide the large stroke. The tuner will be actuated by a customized Phytron LAV stepper motor with a

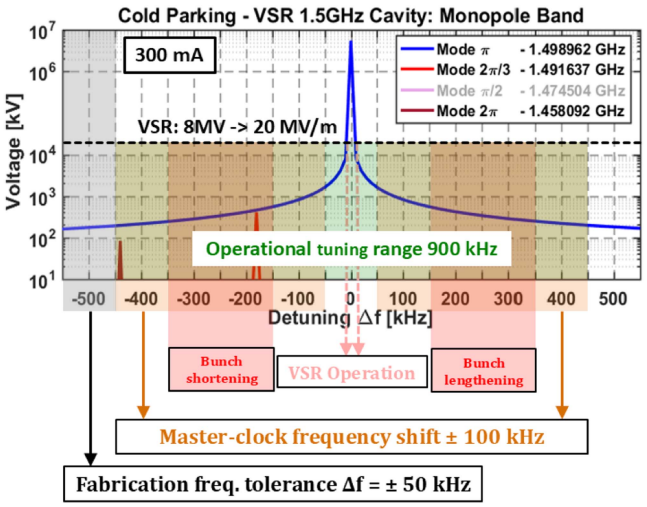

Fig. 11. Cavity tuning range for different operations.

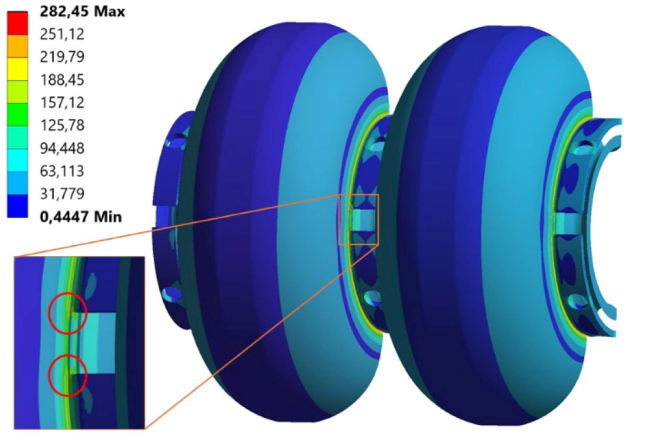

Fig. 12. Peak stress in the contact region of cell and stiffening rings at 1.5 mm tuning. Computational singularities originating in mesh-mismatches of small contacting zones are removed.

50:1 planetary gear. On one side, the blade tuner will be directly mounted onto the cavity's tuner flange, and on the other side, it will be connected to the flange via four intermediate support frames housing the piezos for fast tuning (cf. Fig. 5). The blade tuner operates the cavity in expansion. Hence, the cavity's reaction force and the force from pressure in the cavity vessel (also in cryo-plant failure scenarios) are counteracting, which is important for the tuning system force requirements.

Based on the transmission ratio of the system cavity to tuner to gearbox to stepper-motor, a frequency shift of 2.1 Hz/step can be achieved. This is just meeting the required resolution, while the piezos can cover 4 µm in cold to compensate for microphonics. The required tuning resolution combined with the large tuning range and the demand for frequent changes of operational mode originating in the user requests for the synchrotron machine, the motor must provide an estimate of nearly $30 \cdot 10^6$ steps/year [15]. This large amount of tuning may lead to failure of one of the system's components, with the stepper motor assembly considered the most prone to fail, and intensive testing has been carried out [15].

During installation of the blade tuner and the piezo elements, some pre-tuning has to be applied to the cavity while it is at room temperature. Simulations indicate a sensitivity to tuning of 190 MPa/mm for the elastic regime. The max. permissible pretuning is set to 0.15 mm, yielding a safety factor of 1.4 against plastic deformation.

Simulations revealed that a cavity fully detuned by 1.5 mm at room temperature would experience severe plastic deformations or even ruptures. This could occur in case of a faulty component in the tuning system, preventing the detuning of the cavity before warm-up. The computational results indicate peak stresses of nearly 300 MPa in the contact region of the cells with the stiffening rings for the maximum detuned cavity (cf. Fig. 12), significantly exceeding niobium's ultimate strength at room temperature. With a release mechanism of the tuning system, this overload can be prevented, saving the cavity from severe damage. This failure scenario is considered a major failure case and is not likely to occur more than once. However, due to its severeness, a releasing mechanism needs to be integrated and is in the final design and trial phase [15]. The release mechanism is designed to disconnect the travelling nut on the spindle from its linkage to the tuner lever arm (cf. Fig. 5). The decoupling is accomplished via a separation bolt that can be actuated at cryogenic temperature and is currently undergoing final testing.

To replace such a failed motor, a contingency plan of the following steps would be executed:

1) Trigger of the release mechanism: The blade tuner is disconnected from the motor and hence, no longer tuning the cavity. Cavity detuning is then determined by the pressure inside the helium vessel with a simulated sensitivity of 0.39 mm/bar(a) in the elastic material regime.
2) Cavity warm-up with a dedicated scheme. The max. allowable pressure in the helium system is limited to 0.5 bar(a) to stay below the elastic limit of niobium and to allow for some inaccuracy in the simulation result. In a warm state, the cavity vacuum is vented first before raising the vessel pressure to atmosphere.
3) Venting of the module and access to the motor by dismantling the cold mass from the module (effortful disassembly).

It is apparent that a motor fault would cause a lengthy repair period. The release mechanism and the warm-up scheme with limited peak pressure are unusual and complex measures for a fault case that is unlikely to happen. Nevertheless, these measures are important to save the cavity from plastic deformation, which results in permanent detuning and, hence, makes it most likely unusable.

Peak stress of nearly 300 MPa of the fully detuned cavity also exceeds the allowable stress at cryogenic temperature of 200 MPa set to achieve sufficient safety against rupture and plastic deformation. Taking a closer look at the simulation results, these high stress values are very much concentrated in small areas (contact of stiffening rings and cells, cf. Fig. 12) with welds. Here, simulations may overpredict stress values due to the sharp geometry changes. Therefore, after close examination

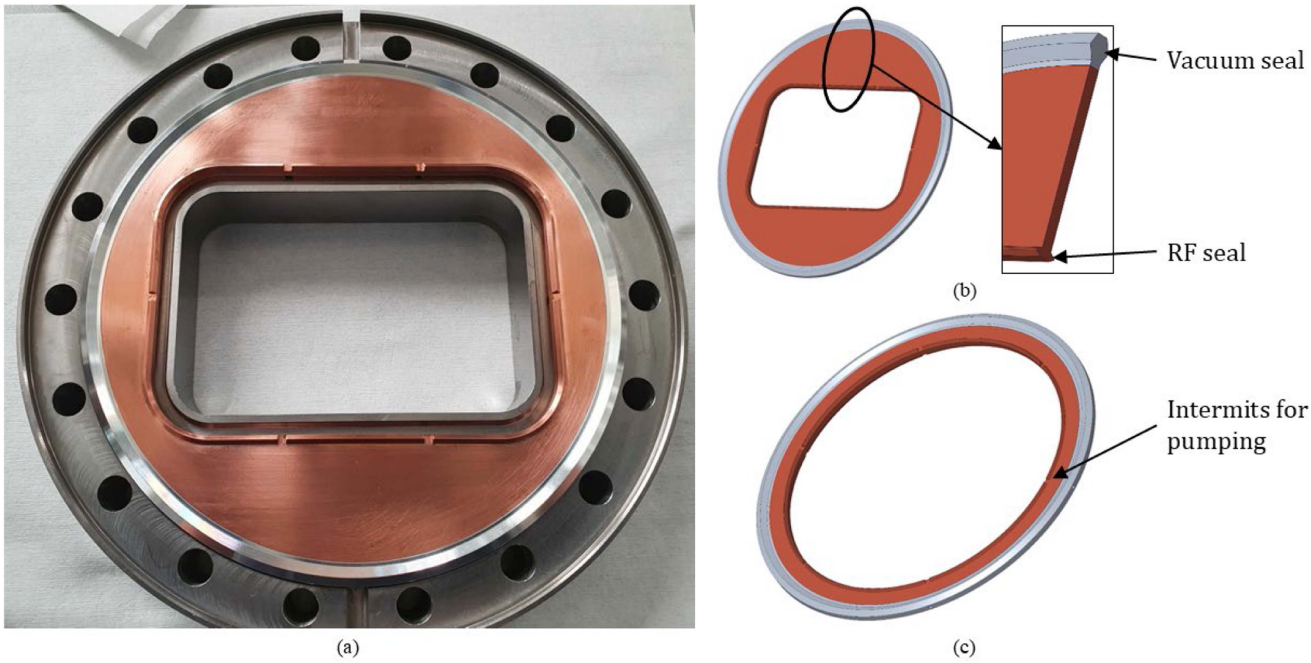

Fig. 13. Gaskets developed for NbTi55 flanges. (a) Waveguide flange prototype with gasket for cold testing. Same gasket design for (b) waveguide and (c) beam pipe flanges with separated RF and vacuum sealing, RF sealing intermitted for vacuum pumping whilst preventing creation of resonating pill-box cavities.

of the simulation results and consultation with the inspection authority, these values are accepted as they occur in very small and limited regions and are considered numerical overestimates.

C. Waveguide Flanges and Gaskets

The cavity design imposed special demands on components considered standard for other designs. During tests in the LVTS, the cavity will be immersed in a superfluid helium bath at 1.8 K. Hence, all shut cavity flanges must be leak-tight to superfluid helium. These flanges comprise of the cavity beam-pipe flanges, the flange connecting the FPC, the actively cooled WG flanges and flanges with pick-ups. All flanges were changed to the same gasket design during the design process.

The flanges on the WG required more engineering, mainly due to the rectangular shape of the inner contour that needed to be sealed. The first design was rectangular [32], following the natural shape of the WGs and minimizing the required space and added weight. Sealing of this design was planned for with a VATSEAL gasket [33] because of the reported successful tests [34]. This flat metal gasket requires a dedicated surface preparation with Ra $=$ 0.2 µm and a geometrical planarity of 0.02 mm over 50 mm. Test pieces were manufactured to test the flange's tightness, and it was found that the demanded surface finish and planarity values were challenging to achieve with NbTi55. Manufacturing costs were high, yet rework was required. Additionally, the cold test performed in HZB's vertical test stand was unsuccessful. It was concluded that this sealing technology is unsuitable for NbTi55 flanges in the environment of supercritical helium.

Thus, the gasketing type was changed to the design used for the beam pipe and coupler port flanges. These customized gaskets consist of an outer circular hexagon-profiled aluminum part (AlMgSi0.5) for vacuum sealing (advantageous over rectangular shape, avoiding unevenly distributed stress with peaks in small radii between the flanks), mated with an OFHC copper insert (see Fig. 13). This insert has a rectangular opening as close as possible to the WG with additional so-called RF lips to achieve the best electrical contact between the WG on the cavity side and the connected copper-coated WG bend. These lips have evenly spaced grooves to allow for vacuum pumping and avoid virtual leakage. For the beampipe and coupler port flanges, the same gasket design is used with round instead of the rectangular cut-out in the copper part. Tests of these gaskets have proven sufficient leak tightness in supercritical helium and food RF performance.

The changed gasketing required re-designing of the WG flanges with a circular outer shape, resulting in a new design of larger size and more weight compared to the initial rectangular flange shape. To verify this design's leak tightness, tests were performed by mating two NbTi55 flanges with one another—as required for cold testing to achieve superconductivity—as well as combining a NbTi55 flange with one out of stainless steel—resembling the final assembly stage of the cavity when the WG bends are connected. Both tests have proven successful with a leak rate of less than $2{\cdot}10^{-10}$ mbar·l/s in both warm (300 K) and cold (4 K) condition.

Operation of the HOMs loads at room temperature imposes a thermal gradient of about 300 K along the WG bend. Thus, to keep the WG extensions of the cavity reliably in a superconducting state, each WG flange has an inner cooling channel connected to the 5–8 K cooling system (see Fig. 14), i.e., [31]. The cooling channel is machined into the flange block, and two pipes enter the outer flange surface through radial holes. A flat

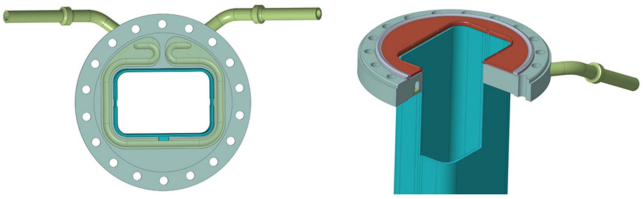

Fig. 14. Cooled waveguide flange (a) bottom view with the covering titanium plate semi-transparent showing the cooling channel, inlet, and outlet pipes; (b) cut view of the flange with gasket and waveguide section.

plate is welded atop the flange to enclose the cooling channel. The flange cooling system operates at 3 bar(a) with a safety valve opening at 15 bar(a). This requires a testing pressure of 22.9 bar(a), i.e., 1.43 times operating pressure as regulated in [21]. Hence, conformity with the rules of pressurized systems is provided; details are to be found in Section III-B.1.

The heavy assembly of WG bends and HOM loads—weight loaded mainly through the flanges and the ceramic tiles for HOM absorption—is connected to the cavity WG flange. To prevent additional weight loading of the WG extension and cavity endgroup, the HOM loads are supported in the space frame to take most of their weight. Simulations have proven that even the blind-flanged WG flanges deadweight is uncritical and neither cause deformations of the WG, the endgroups, nor the welded connection of the WG and helium vessel. However, the WGs and WG flanges will be supported by a dedicated frame for transportation.

III. Manufacturing

A. Bellows Requirements and Protection

The cavity vessel comprises a bellows that is required for tuning during operation. The protruding WGs prevent the bellows from being slid onto the assembly, thus necessitating its inclusion as part of the undressed cavity. This implies that the bellows is present during the heat treatment of the naked cavity at 800 °C, during cavity cell tuning, during transport, and during the cold test. Any damage to the bellows requires a lengthy repair cycle, including dismantling one cavity cell. Consequently, RI designed a special bellows protection to prevent damage during transport, handling, and processing of the cavity. To access all cells for tuning after welding the naked cavity, it is necessary to move the bellows, which otherwise would shade the end-cell.

The bellows is a single-layer titanium with a 0.6 mm wall thickness capable of withstanding an internal pressure of 3.5 bara. The bellows with five corrugations and only 48 mm length allows for a tuning range of 1.5 mm. It survives the max. temperature of 800 °C during heat treatment without degradation.

B. Pressure Vessel Certification

The cavity with vessel is classified as a pressure vessel category smaller than one according to the Pressure Equipment Directive [21] due to size, volume, and maximum pressure. Consequently, the cavity can be manufactured in accordance with the sound engineering practice of the member state Germany ([21] article 4, paragraph 3). Nevertheless, the specific design of the cavity and the cryo plant's release pressure necessitate an assessment of critical manufacturing steps. A third party, DEKRA, is involved in the manufacturing process for quality control and reliability assessment. DEKRA has and will perform and accompany tests of subcomponents and of the assembly. A detailed inspection and test plan [35] was developed in collaboration with the manufacturer and the third party. The plan comprises dedicated material testing regarding material strength and hardness, inspection of welding procedures, welding seams, and tests of welded samples. It also includes pressure tests of subassemblies such as the WG flange and a final pressure test of the fully assembled and dressed cavity at a pressure level of 1.5 bar(a).

Niobium samples of standard shape and dimension [36] are cut from the raw material sheets with different orientations (i.e., 0°, 45°, and 90°). These samples are used to measure Vickers hardness, yield strength, and ultimate strength at room temperature. The material is tested in its as-received state, with welding seams, and after 800 °C heat treatment with and without welding seams. Samples were selected from those sheets with minimum, maximum, and average Vickers hardness, as determined by the material supplier. The test results are summarized in Table V, which also indicates the number of samples evaluated. For each sample group, the minimum and maximum values of yield and ultimate strength are reported, along with the arithmetic mean. Given the small sample size, further statistical analysis was considered not meaningful.

The data in Table V provide insight into the influence of the various processing steps on the material strength. In particular, the results reveal that heat treatment partially recovers strength losses induced by welding, likely due to stress relief during the thermal process. A more comprehensive statistical analysis would require a significantly larger number of samples to reduce uncertainty. Nevertheless, the present measurements indicate that the conservative yield strength value of 38 MPa, reported in [24], is not supported by the current dataset, with the lowest measured yield strength being 44 MPa. For ultimate tensile strength, the minimum measured value was 119 MPa, only marginally higher than the value reported in Table III. Based on these findings, a reassessment of the safety factors is warranted. The updated material properties result in an approximately 15% higher safety margin against plastic deformation at room temperature, while the margin against rupture remains nearly unchanged.

Welding seams are assessed prior to production start by way of example. Once the undressed cavity has been completed, all welding seams need to be inspected visually. The dressed cavity will also be inspected visually, and welding seams on the cavity vessel will undergo eddy-current testing for integrated assessment. The final acceptance of the cavity concerning pressure stability will be performed with pressurized gas inside the helium vessel at a pressure of up to 1.5 bar(a). This value is understood as the max. operation pressure but is below the max. pressure of 3.5 bar(a) in a fault case. However, this would result in plastic deformations of the cavity when occurring at room

TABLE V
STRENGTH VALUES OF THE NIOBIUM MATERIAL AT DIFFERENT STAGES OF THE MANUFACTURING PROCESS

Material treatment		Orientation	Sample size	Yield strength [MPa]			Tensile strength [MPa]		
				Min.	Average	Max.	Min.	Average	Max.
As received		0°	5	73	77.8	84	172	177.2	182
		45°	5	75	76.2	78	169	173.2	176
		90°	6	64	72.8	79	166	171.0	173
800°C bake-out for 3 h		0°	8	54	58.4	63	165	168.7	174
		90°	8	56	56.8	58	159	162.9	168
Welded	weld in pulling direction	-	5	42	48.0	64	106	108.8	111
	weld 90° to pulling direction	-	2	53	54.0	55	107	108.5	110
Welded and 800°C bake-out	weld in pulling direction	-	4	**44**	47.0	50	**119**	122.3	125
	weld 90° to pulling direction	-	4	59	64.0	68	129	138.8	147

Material was taken in different orientations from the sheets. Not all samples tested successfully (insufficient clamping force); only successful samples are reported. Highlighted are the lowest yield and tensile strength values found for the material with heat-treatment and welding seam. Minimum strength exceeds the values taken for design calculations as in TABLE III.

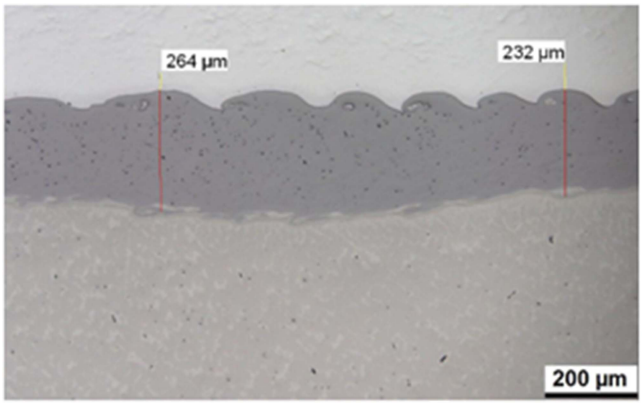

Fig. 15. Microsection inspecting the explosion-bonded transition of titanium and stainless steel.

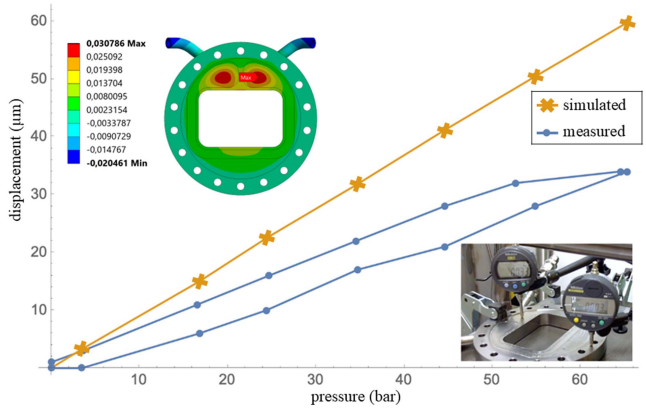

Fig. 16. Pressure testing of the waveguide flange's cooling channel. Measured and simulated deformation values of the welded covering plate. Some hysteresis was observed with stronger deformation during pressure reduction (blue, upper branch) and remaining plastic deformation of 1 µm, which is close to the resolution limit of the gauge.

temperature. Given the rigorous inspection protocol employed during manufacturing, the reduced testing pressure is deemed acceptable.

Semi-finished products purchased from sub-suppliers (e.g., the bellows) undergo a meticulous inspection process, accompanied by the requisite documentation. Due to the limited space and the need to provide a CF edge in stainless steel, an explosion-bonded transition from titanium to stainless steel is inserted in the pipes for cooling media, such as the helium vessel inlet, outlet, and in the cooling pipes of the WG flange. Dedicated testing is conducted on those pipe segments, including visual inspection of microsections (see Fig. 15), permeability measurements, and integral pressure testing.

1) Waveguide Flange Approval: The cooled WG flanges are connected to a secondary cooling circuit operating at 5 K and with a safety valve opening at 16 bar(a). To guarantee the stability and tightness of the cooling channel integrated into the flange body, one prototype flange was tested as an example up to a pressure of 65.3 bar(a), accepting potential plastic deformation if not destruction and even with an overpressure of about four times the operational pressure, plastic deformations remained negligible, even though shape hysteresis during pressure reduction was observed (cf. Fig. 16). All the manufactured flanges

successfully underwent pressure testing up to 22.9 bar (i.e., that is 1.43 times the max. pressure as required) and of leak-tightness.

IV. Conclusion

The unprecedented and complex cavity design that allows for high HOM loading, a large tuning range, and high failure pressure in the cooling system was proven to be operable and safe.

The mechanical design of the 1.5 GHz SRF cavity, equipped with waveguides for efficient HOM damping, was developed from a preliminary concept to a manufacturing-ready level of detail. Adjustments during the late design stage and throughout manufacturing were necessary to facilitate the novel cavity design with protruding waveguides.

The realized enhancements of the pressure stability allow operation in a helium bath at pressures up to 3.5 bar(a). This was made possible by introducing internal ribs within the vessel to reduce bulge effects, modifying the chamfer radius of WGs and FPC port, and by introducing external ribs on the cavity between the WGs. These design optimizations have already been implemented in the prototype cavity currently under production.

A dedicated quality control and testing protocol was developed to accompany the manufacturing process. This approach allows for a final pressure test of the cavity at a lower value than the maximum possible value in a fault case. Tensile tests of niobium samples retrieved at various manufacturing stages revealed that welding induces a comparable or slightly greater degradation in material strength than the 800 °C heat treatment. These tensile tests provided niobium material data that were previously not readily available.

The cavity design shape required innovative solutions. For instance, the vessel-intersecting WGs featuring T-shape inserts with a direct weld of niobium to titanium. And the superconducting WG part outside the helium vessel featuring flanges cooled by 5 K helium. To provide vacuum and RF sealing on NbTi55 flanges, customized gaskets were developed and tested. These gaskets combine a copper and an aluminum part and demonstrated sufficient sealing of the flanges when submerged in supercritical helium.

Now, the manufacturing process is approaching a major milestone with the completion of a first dressed cavity. This prototype cavity features all the afore mentioned improvements. The safety assessment of the undressed prototype cavity was successfully completed, based not only on welding samples and the material samples tested but also approved by a pressure test. Further insights are expected from the upcoming tests of this prototype cavity.

Acknowledgment

The authors would like to thank RI Research Instruments GmbH, in particular, A. Navitski and M. Pekeler for the intensive collaboration during the manufacturing phase. Highly valuable advice — also at very early design stages — based on distinct experience was received from E. Zaplatin and W.-D. Möller.

M. Dirsat supported this work by helping with difficult simulation questions. A. Frahm contributed with his engineering experience and his vigorous approach. Y. Tamashevich assisted the design process with his experience and hands-on, e.g., during flange cold-testing. Finally, the authors would like to thank A. Neumann and V. Dürr for advice on various topics.

References

[1] B. Aune et al., "Superconducting TESLA cavities," *Phys. Rev. Special Top.-Accel. Beams*, vol. 3, no. 9, Sep. 2000, Art. no. 092001, doi: 10.1103/PhysRevSTAB.3.092001.

[2] O. Kononenko, C. Adolphsen, Z. Li, T. Raubenheimer, and C. Rivetta, "Electro-mechanical modelling of the LCLS-II superconducting cavities," in *Proc. 28th Linear Acc. Conf.*, 2016, pp. 310–312, doi: 10.18429/JACoW-LINAC2016-MOP106006.

[3] W. Singer et al., "Production of superconducting 1.3-GHz cavities for the European X-ray free electron laser," *Phys. Rev. Accel. Beams*, vol. 19, no. 9, Sep. 2016, Art. no. 092001, doi: 10.1103/PhysRevAccelBeams.19.092001.

[4] H. Padamsee et al., "Accelerating cavity development for the Cornell B-Facotry, CESR-B," in *Proc. IEEE Part. Accel. Conf.*, 1991, vol. 2, pp. 786–788.

[5] R. Eichhorn et al., "Higher order mode absorber for high current ERL applications," in *Proc. 5th Int. Conf. RF Supercond.*, 2015, pp. 1036–1042, doi: 10.18429/JACoW-SRF2015-THBA05.

[6] R. Eichhorn et al., "Higher order mode absorbers for high current ERL applications," in *Proc. 5th Int. Part. Accel. Conf.*, 2014, pp. 4037–4039, doi: 10.18429/JACoW-IPAC2014-THPRI111.

[7] J. Sekutowicz et al., "Research and development towards duty factor upgrade of the European X-Ray free electron laser linac," *Phys. Rev. Accel. Beams*, vol. 18, no. 5, May 2015, Art. no. 050701, doi: 10.1103/PhysRevSTAB.18.050701.

[8] M. Neubauer et al., "Beam pipe HOM absorbers for SRF cavities," in *Proc. Part. Accel. Conf.*, 2011, pp. 1012–1014.

[9] R. Rimmer et al., "Recent progress on high-current SRF cavities at JLab," in *Proc. 1st Int. Part. Accel. Conf.*, 2010, pp. 3052–3054.

[10] F. Marhauser et al., "Status and test results of high current 5-cell SRF cavities developed at JLAB," in *Proc. EPAC*, 2008, pp. 886–888.

[11] A. Jankowiak, J. Knobloch, P. Goslawski, and A. Neumann, Eds., *Technical Design Study BESSY VSR*. Berlin, Germany: Helmholtz-Zentrum Berlin, 2015, doi: 10.5442/R0001.

[12] A. Jankowiak et al., "The Bessy VSR project for short X-ray pulse production," in *Proc. 7th Int. Part. Accel. Conf.*, 2016, pp. 2833–2836.

[13] J. Guo et al., "Development of waveguide HOM loads for BERLinPro and BESSY-VSR SRF cavities," in *Proc. 8th Int. Part. Accel. Conf.*, 2017, pp. 1160–1163, doi: 10.18429/JACoW-IPAC2017-MOPVA130.

[14] N. Wunderer et al., "VSR demo cold string: Recent developments and manufacturing status," in *Proc. 20th Int. Conf. RF Supercond.*, 2021, pp. 647–651, doi: 10.18429/JACoW-SRF2021-WEPTEV008.

[15] N. Wunderer et al., "Design and testing of the VSR blade tuner and actuators," in *Proc. 14th Int. Part. Accel. Conf.*, 2023, pp. 4412–4415, doi: 10.18429/JACoW-IPAC2023-THPA191.

[16] E. Sharples, M. Dirsat, J. Knobloch, Z. Muza, and A. Velez, "Design development for the 1.5 GHz couplers for BESSY VSR," in *Proc. 19th Int. Conf. RF Supercond.*, 2019, pp. 795–799, doi: 10.18429/JACoW-SRF2019-WETEB9.

[17] V. Veshcherevich et al., "Design of high power input coupler for Cornell ERL injector cavities," in *Proc. 12th Int. Workshop RF Supercond.*, 2005, pp. 590–592.

[18] F. Glöckner et al., "The VSR demo module design – A spaceframe-based module for cavities with warm waveguide HOM absorbers," in *Proc. 20th Int. Conf. RF Supercond.*, 2021, pp. 233–236, doi: 10.18429/JACoW-SRF2021-MOPTEV013.

[19] A. Velez, H.-W. Glock, J. Knobloch, and A. Neumann, "HOM damping optimization design studies for BESSY VSR cavities," in *Proc. 6th Int. Part. Accel. Conf.*, 2015, pp. 2774–2776, doi: 10.18429/JACoW-IPAC2015-WEPMA013.

[20] A. Velez, J. Knobloch, and A. Neumann, "BESSY VSR 1.5 GHz cavity design and considerations on waveguide damping," in *Proc. 27th Int. Linear Accel. Conf.*, 2014, pp. 221–223.

[21] Directive 2014/68/EU of the European Parliament and of the Council of 15 May 2014 on the harmonisation of the laws of the Member States relating to the making available on the market of pressure equipment (recast) Text with EEA relevance, 2014/68/EU, May 2014. [Online]. Available: http://data.europa.eu/eli/dir/2014/68/oj

[22] M. Merio, L. Ristori, and T. Peterson, "Material properties for engineering analyses of SRF cavities," Fermilab, Batavia, IL, USA, Tech. Rep. Fermilab Specification: ED0371110, 5500.000-ES-371110, Rev. A, 2013.
[23] G. Myneni and H. Umezawa, "Variation of mechanical properties of high RRR and reactor grade niobium with heat treatments," *Matériaux Techn.*, vol. 91, nos. 7/9, pp. 19–22, 2003, doi: 10.1051/mattech/200391070019.
[24] T. Peterson et al., "Pure niobium as pressure vessel material," in *Proc. AIP Conf.*, 2010, vol. 1218, no. 1, pp. 839–848, doi: 10.1063/1.3422438.
[25] A. Tsakanian, "Design of the BESSY VSR waveguide damped cavities and ancillary components for the cold string," in *Proc. ICFA Mini Workshop HOMs SRF Cavities*, 2018. Accessed: Apr. 25. [Online]. Availible: https://indico.classe.cornell.edu/event/185/contributions/567/attachments/432/533/HOMSC2018_Tsakanian_Print.pdf
[26] Metalcor GmbH, "Datenblatt 3.7035 Ti-grade 2," Metalcor GmbH. Accessed: Jun. 17, 2024. [Online]. Available: https://www.metalcor.de/datenblatt/122/
[27] M. Praise, D. Passarelli, and J. Bernardini, "Niobium to titanium electron beam welding for SRF cavities," in *Proc. Int. Linear Accel. Conf.*, 2022, pp. 515–518. doi: 10.18429/JACoW-LINAC2022-TUPOGE13.
[28] E. Sharples-Milne, V. Dürr, J. Knobloch, S. Schendler, A. Velez, and N. Wunderer, "The 1.5 GHz coupler for VSR demo: Final design studies, fabrication status and initial testing plans," in *Proc. 20th Int. Conf. RF Supercond.*, 2021, pp. 652–656, doi: 10.18429/JACoW-SRF2021-WEPTEV009.
[29] E. Zaplatin, H.-W. Glock, J. Knobloch, A. Neumann, and A. Velez, "First considerations on HZB high frequency elliptical resonator stiffening," in *Proc. 18th Int. Conf. RF Supercond.*, 2017, pp. 428–432, doi: 10.18429/JACoW-SRF2017-TUPB021.
[30] N. Wunderer, "BESSY VSR 1.5 GHz cavity stiffening ring variation," Helmholtz-Zentrum Berlin, Berlin, Germany, Int. Rep. VSR-PCD-R01137.0, Feb. 2019.
[31] A. Neumann, "BESSY VSR 1.5 GHz cavity stiffening ring options," Helmholtz-Zentrum Berlin, Berlin, Germany, Int. Rep. VSR-SRF-R00743.0, Feb. 2019.
[32] A. Velez et al., "BESSY VSR: SRF challenges and development for a variable-pulse length next-generation light source," in *Proc. 18th Int. Conf. RF Supercond.*, 2017, pp. 29–35, doi: 10.18429/JACoW-SRF2017-MOYA02.
[33] VAT Group AG, "Vakuumventil-technologien – VATSEAL," Accessed: Apr. 10, 2025. [Online]. Available: https://www.vatgroup.com/de/vacuum-valves/vacuum-valves-technologies
[34] S. Vilcins, D. Bandke, and M. Holz, "A new sealing technology for high precision wide open UHV vacuum flange and waveguide connections with metal gaskets," in *Proc. 10th Mech. Eng. Des. Synchrotron Radiat. Equip. Instrum.*, 2018, pp. 125–128, doi: 10.18429/JACoW-MEDSI2018-TUPH37.
[35] N. Wunderer and K. Weber, "VSR cavity pressure vessel certification steps including the draft Inspection and Test plan," Helmholtz-Zentrum Berlin, Berlin, Germany, Int. Rep. VSR-SRF-S00862.5, Nov. 2020.
[36] Metallic Materials – Tensile Testing – Part 1: Method of Test at Room Temperature, ISO 6892-1:2019, 2020, doi: 10.31030/3132591.